Improving aeration systems in saline water (part II): effect of different salts and diffuser type on oxygen transfer of fine-bubble aeration systems

J. Behnisch, M. Schwarz, J. Trippel, M. Engelhart and M. Wagner

ABSTRACT

The objective of the present study is to investigate the different effects on the oxygen transfer of fine-bubble aeration systems in saline water. Compared to tap water, oxygen transfer increases due to the inhibition of bubble coalescence. In Part I of the present study, we investigated in laboratory-scale experiments the effect of design of diffuser membrane. The objective of Part II is the assessment of effects of different salts, diffuser type and diffuser density. We measured the concentration of various salts ($MgCl_2$; $CaCl_2$; Na_2SO_4; NaCl; KCl) above which coalescence is fully inhibited and oxygen transfer reaches its maximum (referred to as the critical coalescence concentration; CCC). For this purpose, we developed a new analytical approach, which enables investigation of the coalescence behaviour of any aeration system and (mixed) salt solution quickly and easily by evaluating the results of oxygen transfer tests. To investigate the transferability to large scale and the effect of diffuser type and density, we repeated lab-scale experiments in a 17,100 L pilot-scale test tank and carried out additional tests with tube and plate diffusers at different diffuser densities. The results show that despite the higher pressure drop, diffusers with dense slit density and smaller slits are to be recommended in order to improve efficiency of aeration systems in saline water.

Key words | critical coalescence concentration, flexible membrane diffuser, SAE, SSOTE, transition concentration

J. Behnisch (corresponding author)
M. Schwarz
J. Trippel
M. Engelhart
M. Wagner
Technical University of Darmstadt, Institut IWAR, Franziska-Braun-Str. 7, 64287 Darmstadt, Germany
E-mail: *j.behnisch@iwar.tu-darmstadt.de*

HIGHLIGHTS

- First time measurement of critical coalescence concentration (CCC) of various salts with fine bubble diffusers.
- New analytical approach for measurement CCC.
- Assessment of effects of different salts, diffuser type and diffuser density on oxygen transfer.
- Additional design consideration for aeration in saline water.

INTRODUCTION

Today, in biological wastewater treatment plants, mainly fine-bubble aeration systems are used to satisfy the oxygen demand of microorganisms in activated sludge (Wagner & Stenstrom 2014). Air is introduced via diffusers installed at the bottom of the aeration tank. From the rising air bubbles, the oxygen is transferred to the liquid phase. There are different diffuser types available (discs, plates, tubes) made out of various materials. Oxygen transfer from ascending air bubbles to the liquid phase is described by the volumetric mass transfer coefficient (k_La), which represents

doi: 10.2166/wst.2021.185

the product of the liquid-side mass transfer coefficient (k_L) and the liquid/gas interfacial area (a). The k_La mainly depends on water quality parameters (e.g. salt concentration, temperature) and diffuser design. Today, mainly some industrial wastewaters show increased salt concentration (Lefebvre & Moletta 2006; He *et al.* 2017). Nevertheless, the global trend towards saving fresh water, e.g. through (industrial)-wastewater reuse or by using seawater for toilet flushing (Sander 2018), will raise the volume of saline wastewater that needs to be (biologically) treated. Depending on the origin of the wastewater, the dissolved salt and salt mixture will change. Therefore, a deeper understanding of the effects of increased concentration of different salts and salt mixtures is crucial to enhance the (energy) efficiency of aerobic biological wastewater treatment.

For fine-bubble aeration systems, increased salt concentration (c_{Salt}) reduces k_L but increases a due to the inhibition of bubble coalescence. The increase is enough to result in a net increase of k_La (Baz-Rodríguez *et al.* 2014). The increase of k_La in saline water (SW) is described by the f_S value, which is the ratio between k_La in SW to k_La in tap water (TW). In Part I of the present work, we could show in laboratory-scale experiments with different conventional disc diffusers by combining bubble size measurement and oxygen transfer tests, that the length and density of the slits in the diffuser membrane influences f_S (Behnisch *et al.* 2018). In this case, the smaller the bubbles detaching from the diffuser (primary bubbles) the higher is f_S. In the early 1980s, Zlokarnik (1980) investigated the coalescence behaviour of different aeration devices commonly used at that time. He also concluded that the more the coalescence is inhibited, the more advantageous it is to use aeration devices, which produce small primary bubbles. Sander *et al.* (2017) carried out oxygen transfer tests at varying sea salt concentrations with disc diffusers in a pilot-scale test tank. They found the simple relationship $f_S = k \cdot c_{Salt} + 1$, whereby k mainly depends on the airflow rate per disc diffuser. Nevertheless, f_S does not increase infinitely. At a certain c_{Salt}, the coalescence is completely inhibited and f_S reaches its maximum ($f_{S,max}$). This concentration is called the critical coalescence concentration (*CCC*) and is specific for each salt (solution) and bubble formation system (Cho & Laskowski 2002; Firouzi *et al.* 2015). Sovechles & Waters (2015) and Quinn *et al.* (2014) determined the *CCC* of varying salts in a lab-scale flotation cell by measuring the bubble size (given as Sauter mean diameter (d_{32})) via image analyses of the bubble swarm at different c_{Salt}. Due to the inhibition of bubble coalescence with increasing c_{Salt}, d_{32} decreases linearly (Zone 1) up to *CCC* (Grau *et al.* 2005). Here (Zone 2), d_{32} reached its minimum ($d_{32,min}$), called the quasi-static-bubble diameter or initial bubble diameter (Marrucci & Nicodemo 1967; Sovechles & Waters 2015). According to Grau *et al.* (2005), the point at which the fitted lines for Zone 1 and Zone 2 meet defines the *CCC*. There are other methods to investigate the coalescence of a system than with image analyses. Craig *et al.* (1993) measured the coalescence by detecting the change of light intensity from an expanded beam of light, which was passed through the bubble swarm produced by a sinter at the base of the transparent test column. Prince & Blanch (1990) used a model-based approach to predict *CCC* for different salts using test results of Marrucci & Nicodemo (1967) and Lessard & Zieminski (1971). While Marrucci & Nicodemo (1967) also applied image analyses to determine the bubble size in a bubble swarm produced by a bronze porous plate, Lessard & Zieminski (1971) observed bubble pairs detaching at the end of two adjacent capillaries. Similar to *CCC*, some researchers also use the transition concentration (TC_X) to quantify the grade of decrease of bubble size with increasing c_{Salt}. The index X indicates the grade at which the bubble size reduces X% from that in pure water to the constant bubble size at high salt concentration. Accordingly, TC_{100} and *CCC* are synonymous (Sovechles & Waters 2015). Currently, there is no definitive agreement explaining the inhibiting effect of salts on bubble coalescence. Firouzi *et al.* (2015) gives a detailed review of all proposed theories, which include colloidal forces, gas solubility, Gibbs-Marangoni effect, surface rheology and ion specific effects.

Experiments show that bubble formation, as well as bubble size, affect *CCC* (Firouzi *et al.* 2015; Sander 2018). Since the bubbles in a flotation cell, as used by Sovechles & Waters (2015), are very small and are formed by cavitation and not by a diffuser, the validity of the results for fine-bubble diffusers is questionable. Furthermore, to investigate the influence of salt on oxygen transfer, previous studies used only disc diffusers (Sander *et al.* 2017; Behnisch *et al.* 2018) or porous plates and frits (Marrucci & Nicodemo 1967; Zlokarnik 1980), which are no longer used today for wastewater treatment. Additionally, only the influence of NaCl and sea salt has been investigated so far.

Therefore, we determined for the first time *CCC* for different salts with conventional fine-bubble diffusers. Because measuring bubble size in a bubble swarm is laborious, we transferred the method of Grau *et al.* (2005) for determining *CCC* to our results of oxygen transfer tests. To do so, we took advantage of the fact that f_S behaves similarly to d_{32} with increasing c_{Salt}, only with reversed sign. The f_S value increases linearly instead of a linear decrease in d_{32}.

In order to investigate the transferability of the results to large scale as well as the influence of the diffuser type and diffuser density on f_S, we also carried out oxygen transfer tests with disc, tube and plate diffusers in a 17,100 L fully glazed steel frame tank at c_{Salt} between 0 and 20 g/L NaCl. Finally, we show the large improvement of aeration in SW by comparing specific standard oxygen transfer efficiency (*SSOTE*) and standard aeration efficiency (*SAE*) with TW conditions, and give some additional design considerations.

MATERIALS AND METHODS

Membrane diffusers

Six different conventional membrane diffusers (2 disc diffusers, 2 plate diffusers, 2 tube diffusers) with different slit densities (*SD*) and slit lengths (d_S) were used (Table 1). *SD* is defined as the number of slits relative to the active (perforated) membrane area (A_A). In the tube diffusers used here, perforation is only on the side of the diffuser and the top and bottom are not perforated (Figure 1). For plates and discs, A_A is similar to the projected media surface area (A_P). Depending on the percentage of perforated membrane area, for tube diffusers $A_A \gg A_P$ applies. According to Behnisch *et al.* (2020), diffuser density (*DD*) is the total membrane area (including unperforated area) divided by area of the tank floor.

Measuring salt concentration (c_{Salt})

Determining the exact salt concentration during the tests, especially in the large pilot-scale test tank, faced us with some challenges. Large amounts of salt were needed to achieve the desired concentrations (up to 342 kg for a single test). Additionally, the tests for each salt or diffuser type required several days and a regular addition of TW was necessary to compensate for evaporation losses. To ensure constant experimental conditions, an on-line measurement of salinity was necessary. Therefore, we decided to apply a method commonly used in environmental technology and determined c_{Salt} by measuring the conductivity (*EC*) on-site standardized at 20 °C water temperature with standard conductivity cell (TetraCon® 324, WTW, Germany).

The correlation between *EC* and c_{Salt} is usually expressed by a simple linear equation: $c_{Salt} = t \cdot EC$. However, the relationship between *EC* and c_{Salt} is not always linear and depends on the activity of specific dissolved ions, ionic strength (*IS*) and the average activity of all ions in the liquid (Rusydi 2018). Therefore, before starting oxygen transfer tests, we measured *EC* of salt solutions with a known concentration in a 500 mL beaker. Our results show that the relationship in the chosen concentration ranges is always linear. This can be seen, for example, in the calibration line for $MgCl_2$ in Figure 2(a). Therefore, the calibration line is given by the following formula: $EC = b_1 \cdot c_{Salt} + b_0$, b_0 being the *EC* of TW. In all our tests, the *EC* of TW was 0.7 mS/cm. With the known calibration lines, we were able to calculate the salt concentration by measuring *EC* on site during oxygen transfer tests. When measuring *EC* in aerated tanks, care must be taken since air bubbles can lead to incorrect measurements.

Measuring CCC with oxygen transfer tests in laboratory-scale experiments

To measure *CCC* for different salts, oxygen transfer tests were performed with *Disc 1* in a rectangular tank (0.5 m × 0.5 m) with a water depth of 1.0 m, using the pure oxygen

Table 1 | Properties of the tested diffusers

Name	Material	A_A [cm²] per diffuser	A_P [cm²] per diffuser	d_S [mm]	P_R/d_S [–]	P_S/d_S [–]	SD [slits/cm²]	slits per diffuser [–]	$q_{A,xxx}$ operation range
Disc 1	EPDM	324	550	0.75	4.07	2.15	15.5	5,028	1.5–8.0[a]
Disc 2	EPDM	306	550	1.25	2.44	1.80	10.0	3,063	1.5–8.0[a]
Plate 1	EPDM	1,867	2,000	0.7	14.3	14.3	0.88	1,636	1.0–3.0[b]
Plate 2	EPDM	1,867	2,000	1.2	2.50	3.75	5.5	10,285	25.0–35.0[b]
Tube 1	Silicon	1,450	665	0.6	3.30	3.33	14.5	21,031	1.0–6.0[c]
Tube 2	Silicon	1,450	665	1.2	1.70	2.08	11.3	16,317	4.0–8.0[c]

EPDM: Ethylene-Propylene-Dien-Terpolymere; A_A: active (perforated) membrane area per diffuser; A_P: projected media surface area per diffuser; d_S: slit length; P_R: distance between rows; P_S: distance between slits; SD: slit density.
Operation range given by manufacturer in: [a]$q_{A,Disc}$ in (m³/h/disc); [b]$q_{A,Plate}$ in (m³/h/plate); [c]$q_{A,Tube}$ in (m³/h/m).

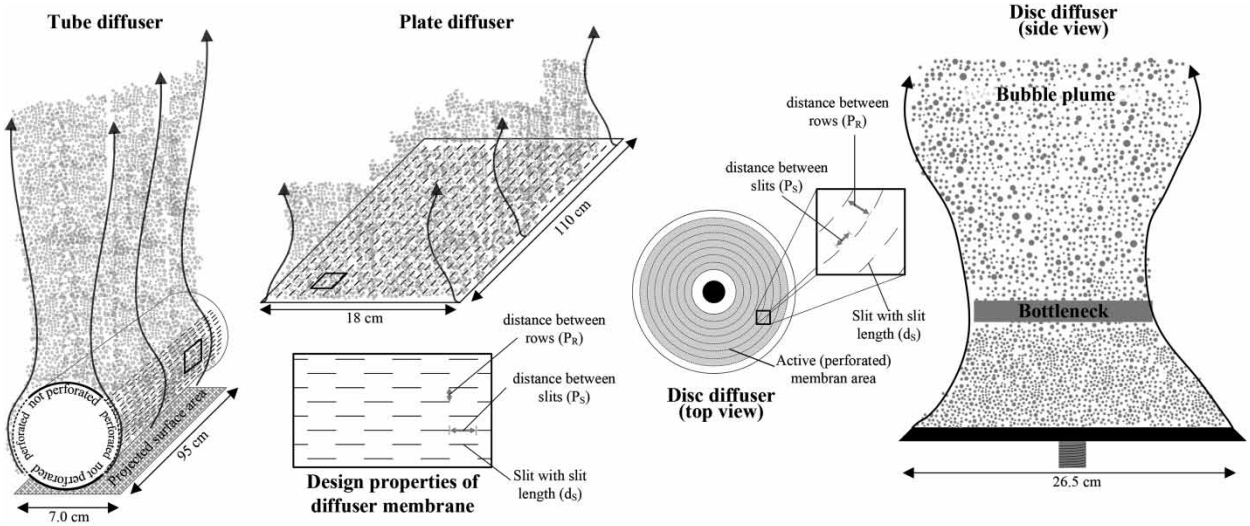

Figure 1 | Schematic representation of the tested diffuser types and the definition of parameters of membrane design.

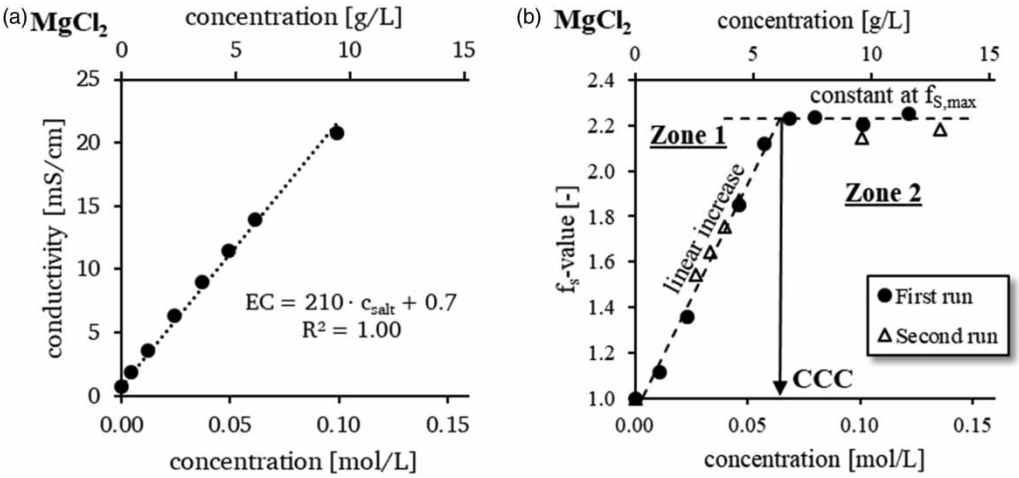

Figure 2 | Measuring CCC: calibration line for calculating $MgCl_2$ concentration by measuring conductivity (a); determining *CCC* of $MgCl_2$ by oxygen transfer test results in lab-scale experiments (b).

desorption method according to EN 12255-15 (2003). With this method, the oxygen concentration is increased 15–20 mg/L beyond the oxygen saturation concentration by aerating with pure oxygen gas or oxygen-enriched air (Wagner *et al.* 1998). By switching to aeration with ambient air, the oxygen concentration starts to decrease again until the saturation concentration is reached. From the curve of decreasing oxygen concentration, the k_La for a specific water temperature (T) is calculated (k_La_T) by nonlinear regression. Four electrochemical oxygen probes (Oxymax COS51D, Endress + Hauser, Germany) were installed to record dissolved oxygen concentration. Finally, the k_La was standardized to 20 °C (k_La_{20}) according to the equation: $k_La_{20} = k_La_T \cdot 1.024^{(20-T)}$.

Tests were performed at different airflow rates (2.0, 3.5 and 4.5 m^3/h) and salt concentrations. The airflow rate was measured at standard temperature and pressure (0 °C; 101.3 kPa; 0% humidity) with a thermal flow sensor (TA16, Hoentzsch, Germany). The $d_{32,min}$ was only measured during tests with NaCl by image analyses (Behnisch *et al.* 2018). Several experiments show that regardless of salt type, the minimum bubble size is always the same (Lessard & Zieminski 1971; Quinn *et al.* 2014). The first test was carried out in TW, then salt was added.

Figure 2(b) shows how *CCC* was determined using the example of test results with $MgCl_2$. According to the method we adapted from Grau *et al.* (2005), the *CCC* results from intersection of the fitted lines of Zone 1 (linear increase of f_S) and Zone 2 (constant f_S at $f_{S,max}$). Accordingly, *CCC* for $MgCl_2$ (CCC_{MgCl2}) is 0.065 mol/L or 6.2 g/L. To verify the reproducibility of the measurement, we repeated the experiment with a new disc diffuser of the same design. In the second run, we measured a CCC of 0.061 mol/L or 5.8 g/L, which represents a deviation of 6%. Therefore, the reproducibility of the results was good.

Oxygen transfer tests in pilot-scale test tank

The pilot-scale test tank is a fully glazed steel frame tank (L/W/H = 3.0 m/1.5 m/4.0 m) with a water level of 3.8 m, yielding a water volume of 17.1 m^3. Ten test series with different diffuser types (Figure 1) and diffuser densities were carried out in the test tank. Therefore, 32 or 6 disc diffusers, 10 or 6 tube diffusers and 4 plate diffusers were installed in the glass tank, respectively. Diffuser depth of submergence was on average 3.65 m and varied negligibly between the individual diffusers.

The oxygen transfer was measured as before in the lab-scale experiments by using the desorption method according to EN 12255-15 2003. As before during lab-scale experiments, dissolved oxygen in water is measured using four electrochemical oxygen probes (Oxymax COS51D, Endress + Hauser, Germany) installed at different positions in the test tank. The compressed air is produced by means of a positive displacement blower (GMA 10.0, Aerzener Machine Factory, Germany). To measure the airflow rate precisely, a calibrated rotary-piston gas meter (Aerzener G 65, type ZB 039.0, Aerzener Machine Factory, Germany) with manometer and thermometer was installed downstream of the blower. The airflow rate (Q_A) was normalized at standard temperature and pressure conditions (0 °C; 101.3 kPa; 0% humidity). Q_A is indicated per aerated tank volume ($Q_{A,VAT} = Q_A \cdot$ (tank volume)$^{-1}$), per disc diffuser ($q_{A,Disc} = Q_A \cdot$ (number of disc diffusers)$^{-1}$), per plate diffuser ($q_{A,plate} = Q_A \cdot$ (number of plate diffusers)$^{-1}$), per length of tube diffuser ($q_{A,tube} = Q_A \cdot$ (number of tube diffusers · length of single tube diffuser)$^{-1}$) or per slit of diffuser membrane ($q_{A,slit} = Q_A \cdot$ (number of diffusers · slits per diffuser)$^{-1}$).

Tests were performed at different airflow rates and NaCl-concentration (c_{NaCl}). The airflow rate set during the tests depends on operational range of diffuser specified by the manufacturer and the capacity of the blower. As described before, c_{NaCl} was calculated by measuring *EC*. Also, the standard oxygen transfer rate per aerated tank volume ($SOTR_{VAT} = \mathrm{SOTR} \cdot$ (aerated tank volume)$^{-1}$) was calculated, *SOTR* being the standard oxygen transfer rate normalized to 20 °C water temperature and atmospheric pressure of 101.3 kPa (EN 12255-15 2003). Here it must be noted, that the solubility of oxygen (c_S) decreases with increasing c_{Salt}. The oxygen saturation concentration for different temperatures and salt concentrations can be taken from tables, to be found e.g. in ISO 5814 2012. According to ASCE/EWRI 18-18 2018, c_S in SW ($c_{S,SW}$) can also be estimated with known c_S in TW ($c_{S,TW}$) and c_{Salt} (in g/L) as follows: $c_{S,SW} = (1.0–0.01 \cdot c_{Salt}) \cdot c_{S,TW}$. However, when comparing $c_{S,SW}$ calculated according to the given formula and the tabulated values, we found an increasing deviation with increasing c_{Salt} (see Annex 1). Therefore, we have adjusted the formula to calculate $c_{S,SW}$ as follows: $c_{S,SW} = (1.0–0.0059 \cdot c_{Salt}) \cdot c_{S,TW}$.

RESULTS AND DISCUSSION

Laboratory-scale experiments

In Table 2 determined dependencies between *EC* and salt concentration are listed. The coefficients of determination

Table 2 | Determined dependencies between EC and salt concentration $EC = b_1 \cdot c_{Salt} + b_0$

Salt	Manufacturer	Assay	b_1 [(mS · L)/(cm · mol)]	b_0 [mS/cm]	R^2 [–]	n [–]	c_{max} [mol/L]	[g/L]
$MgCl_2$	Zschirmer & Schwarz GmbH	94.5%	210	0.7	1.00	7	0.12	11.4
NaCl	Carl Roth GmbH	99.5%	98	0.7	1.00	8	0.35	20.6
KCl	Merck KGaA	99.5%	119	0.7	1.00	12	0.53	39.9
$CaCl_2$	Zschirmer & Schwarz GmbH	94.0%	172	0.7	0.99	8	0.26	28.9
Na_2SO_4	Zschirmer & Schwarz GmbH	99.5%	139	0.7	0.98	8	0.36	51.0

EC: conductivity (mS/cm); c_{Salt}: salt concentration (mol/L); n: number of measuring points; c_{max}: maximum salt concentration at which EC was determined (mol/L or g/L).

(R^2) close to 1.0 prove the linear dependence between *EC* and c_{Salt} within the chosen concentration range up to maximum selected salt concentration (c_{max}). As previously mentioned, the relationship is influenced by many factors, and therefore the equations shown here are only valid in TW for the specified concentration ranges. To calculate the salt concentration in solutions with other background contamination (i.e. dissolved substances other than the salt to be measured), the equation may have to be adapted.

Results in Table 3 summarize the determined *CCC* for different salts together with values given in literature supplemented by information of the observed $d_{32,min}$, test setup and measurement method of coalescence. Regardless of salt type, $f_{S,max}$ reached during *CCC* measurement varied marginally and was on average 2.2. This confirms several experimental studies (Lessard & Zieminski 1971; Quinn *et al.* 2014), which show that in coalescence inhibited systems, k_La and bubble size reach a fixed value regardless of salt type. During the tests of Sander *et al.* (2017), the bubble size was not measured and is therefore not available (n.a.). However, since similar fine-bubble diffusers were used, we can assume that similar bubble sizes were achieved as in our tests.

A direct comparison of the *CCC* reported in the different papers is not possible due to the different measurement methods and test conditions. Nevertheless, some tendencies can be identified. For example, with the exception of Na_2SO_4, the *CCCs* reported by other authors are higher than our results. Only the *CCC* determined by Prince & Blanch (1990) are lower, except for KCl. A possible correlation can be seen here with the observed bubble size, which is larger in the case of Prince & Blanch (1990) and smaller in the case of the other papers than in our own experiments. Already, Firouzi *et al.* (2015) and Sander (2018) showed that the smaller the bubbles the higher the *CCC* of a salt. If only the *CCC* is considered as the molar concentration (i.e. in mol/L) of the salts investigated in all the different studies, the following order emerges for most

Table 3 | Summary of CCC from own measurements and literature references

	own results			Sovechles & Waters (2015)			Quinn *et al.* (2014)			Craig *et al.* (1993)			Prince & Blanch (1990)		
$d_{32,min}$	1.25 mm			0.60 mm			0.60 mm			n.a.			3.6–4.1 mm		
System	Bubble swarm			Bubble swarm			Bubble swarm			Bubble swarm			Bubble pairs/bubble swarm		
Method	oxygen transfer			measuring bubble size			measuring bubble size			turbidity			measuring bubble size		
Bubble formation	Membrane diffuser			Flotation cell			Flotation cell			Sinter plate			Needles/porous plate		
Salt	CCC [mol/L]	CCC [g/L]	IS [–]	CCC [mol/L]	CCC [g/L]	IS [–]	CCC [mol/L]	CCC [g/L]	IS [–]	CCC [mol/L]	CCC [g/L]	IS [–]	CCC [mol/L]	CCC [g/L]	IS [–]
$MgCl_2$	0.063	6.0	0.19	0.092	8.8	0.28				0.086	8.2	0.26	0.055	5.2	0.17
$CaCl_2$	0.080	10.0	0.27	0.091	10.1	0.27	0.11	12.2	0.33	0.17	18.9	0.51	0.055	6.1	0.17
Na_2SO_4	0.085	12.8	0.27	0.082	11.6	0.25	0.13	18.5	0.39				0.061	8.7	0.18
NaCl	0.18	10.5	0.18	0.22	13.1	0.22	0.31	18.1	0.31	0.23	13.4	0.23	0.18	10.2	0.18
KCl	0.21	15.7	0.21	0.25	18.8	0.25	0.31	23.1	0.31	0.33	24.6	0.33	0.23	17.2	0.23
$MgSO_4$				0.071	8.5	0.28	0.070	8.4	0.28	0.090	10.8	0.36	0.032	3.9	0.13
$AlCl_3$				0.056	7.5	0.34									
$Al_2(SO_4)_3$				0.024	8.2	0.35									
NaBr													0.22	22.6	0.22
K_2SO_4													0.080	13.9	0.24
KOH													0.17	9.5	0.17
$CuSO_4$													0.070	11.2	0.28
KI													0.62	102.9	0.62
KNO_3													0.41	41.5	0.41
Sea Salt	*[0.32*	*10*	*0.19]*[a]	0.39	12.4	0.27									

$d_{32,min}$: minimum bubble diameter (also 'quasi-static-bubble diameter' (Marrucci & Nicodemo (1967)) or 'limiting bubble size' (Sovechles & Waters (2015)).
[a]results from Sander *et al.* (2017), $d_{32,min}$ = n.a.
CCC: Critical Coalescence Concentration [in mol/L or g/L]; IS: Ionic Strength [–].

of the studies reported here:

$$MgCl_2 < CaCl_2 < Na_2SO_4 < NaCl < KCl$$

Already, Sovechles & Waters (2015) showed that *CCC* decreases for salts containing multivalent ions. While 1:1 (cation:anion charge) salts had the highest *CCC*; 1:2 and 2:1 salts had intermediate *CCC*; and 2:2, 3:1 and 3:2 salts had the smallest CCC. Therefore, they try to describe the inhibition of coalescence by salt (and multicomponent salt solutions) by calculating *IS*. In analogy to *CCC*, they postulated that coalescence is completely inhibited in their flotation cell when $IS = 0.28$, which they called Critical-Coalescence Ionic Strength (*CCIS*). To verify this, all results in Table 3 were supplemented by the *IS* we calculated. *IS*-values of salt solution by Prince & Blanch (1990) varies between 0.13 and 0.62. Also for our test results, *IS* fluctuates between 0.18 and 0.27. This variation is very large, which is why we cannot confirm the approach postulated by Sovechles & Waters (2015) to describe coalescence inhibition by determining the *IS*. Indeed, the *CCC* must be determined for each new (bubble formation) aeration system individually.

So even if the absolute values of the determined *CCC* do not match those from the literature, which is due to the different bubble size, it can still be said that they are in a specific order relative to each other, independent of the aeration system and the measurement method. The validity of the determined *CCC* and thus of the new measurement method is therefore given.

Experiments in pilot-scale test tank

In the following, first we will present the results of the tests in the pilot-scale test tank for each individual diffuser type. Then we try to consider all the results together and discuss the different effects on f_S more in detail. At the end, we will discuss other parameters that have to be taken into account in design of aeration systems in SW in addition to k_La (or f_S).

Results from disc diffuser

In Figure 3 f_S-values from test series with disc diffusers are plotted against c_{NaCL} for different airflow rates together with the results from lab-scale experiments described in Part I of the present paper (Behnisch *et al.* 2018). For *Disc*

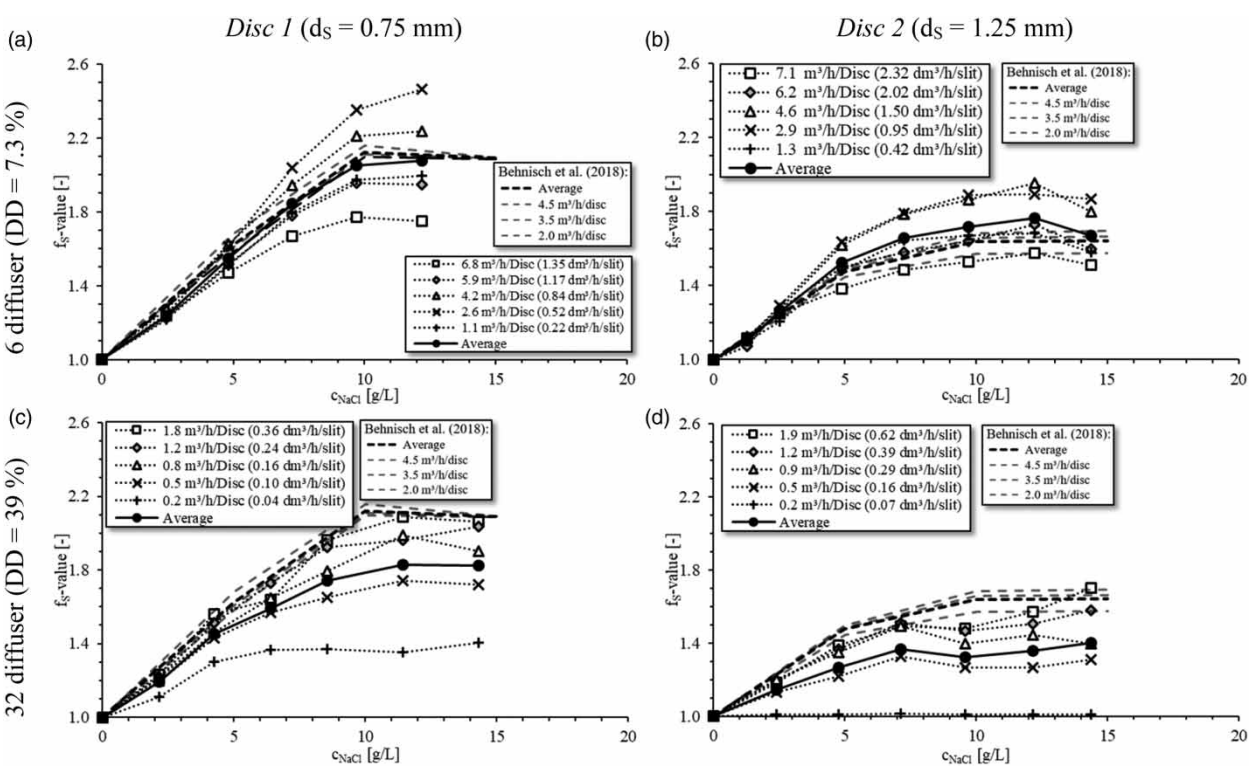

Figure 3 | f_S-values as function of c_{NaCl} from disc diffusers for different $q_{A,Disc}$ and $q_{A,Slit}$ supplemented by results of lab-scale experiments described in Part I of the present paper.

1 f_S increases up to 10 g/L NaCl, which corresponds to the *CCC* of NaCl (CCC_{NaCl}) previously determined in the lab-scale experiments. Then f_S reaches its peak value ($f_{S,max}$). The same is true for *Disc 2*, although the transition point from Zone 1 (linear increase) to Zone 2 (constant value) is not as obvious as with *Disc 1*. The pilot-scale experiments show, that for both disc diffusers, the level of $f_{S,max}$ is strongly dependent on $q_{A,Disc}$. The highest f_S values could be reached in the middle of the operation range (3.0–4.0 Nm^3/h per diffuser) given by the diffuser manufacturer (1.5–8.0 Nm^3/h per diffuser) which corresponds to the results of Sander *et al.* (2017). In case of *Disc 2* at very low $q_{A,Disc}$ of 0.2 m^3/h/disc (Figure 3(d)), f_S is only about 1.0. This means that no salt effect can be observed at such low $q_{A,Disc}$ values. The reason for this will discussed below in the present paper, when discussing the influence of airflow rate on f_S.

Comparing the results of both disc diffusers shows that higher $f_{s,max}$ values were reached with *Disc 1* than with *Disc 2*. Considering the results when the full range of airflow rate was tested (Figure 3(a) and 3(b)), mean $f_{S,max}$ of *Disc 1* (2.0) is 10% higher than of *Disc 2* (1.8). In comparison, k_La_{20}-values in TW are in a comparable range for both diffusers (Annex 2). This confirms the results of previous lab-scale experiments with similar disc diffusers (Behnisch *et al.* 2018). Accordingly, higher f_S values could be reached with smaller slit lengths (*Disc 1* superior to *Disc 2*). Nevertheless, the effect of airflow rate on f_S was not as obvious as in the experiments conducted in the pilot-scale test tank, because of the limited blower capacity and reactor volume during the lab-scale experiments. Consequently, a scale effect has to be taken into account in order to obtain adequate results during measurement of oxygen transfer in SW. A sufficient reactor volume as well as blower capacity is necessary to ensure that the full range of airflow rate of diffusers can be set during the tests. If only two diffusers have to be compared relative to each other, a small reactor is sufficient, whereby the test conditions must be identical.

If both the f_S value and the k_La value rises, so does the $SOTR_{VAT}$. While in *TW* there is a linear relationship between $SOTR_{VAT}$ and $Q_{A,VAT}$ (Behnisch *et al.* 2020), this is not the case in *SW* due to the dependence of f_S (or k_La) on $q_{A,Disc}$. At a salt concentration of 12 g/L NaCl and a $Q_{A,VAT} = 1\ Nm^3/m^3/h$, almost similar $SOTR_{VAT}$ of 123 $g/m^3/h$ and 132 $g/m^3/h$ could be achieved with 6 and 32 *Disc 1* diffusers respectively. This represents an increase of 24% (99 $g/m^3/h$) and 45% (91 $g/m^3/h$) compared to 6 and 32 *Disc 2* diffusers respectively. Compared to $SOTR_{VAT}$ in *TW* it is an increase of 105% (6 diffusers: 60 $g/m^3/h$) or 60% (32 diffusers: 84 $g/m^3/h$). The results show that due to the influence of $q_{A,Disc}$ on f_S, it is possible that in SW with the same $Q_{A,VAT}$ but a different number of diffusers, due to the higher f_S-value (or k_La), similar or even more oxygen can be transferred at low than at high diffuser density.

Results from plate diffuser

In Figure 4, f_S-values from test series with plate diffusers are plotted against c_{NaCl} for different airflow rates. Unexpectedly, there are big differences compared to the results of the disc diffusers. For *Plate 1* (Figure 4(a)), f_S increases up to a concentration of 5 g/L NaCl, which is quite lower than the measured CCC_{NaCl} in lab-scale experiments. Furthermore, the measured $f_{S,max}$ for *Plate 1* is lower than for *Plate 2* (Figure 4(b)), even though *Plate 1* has smaller

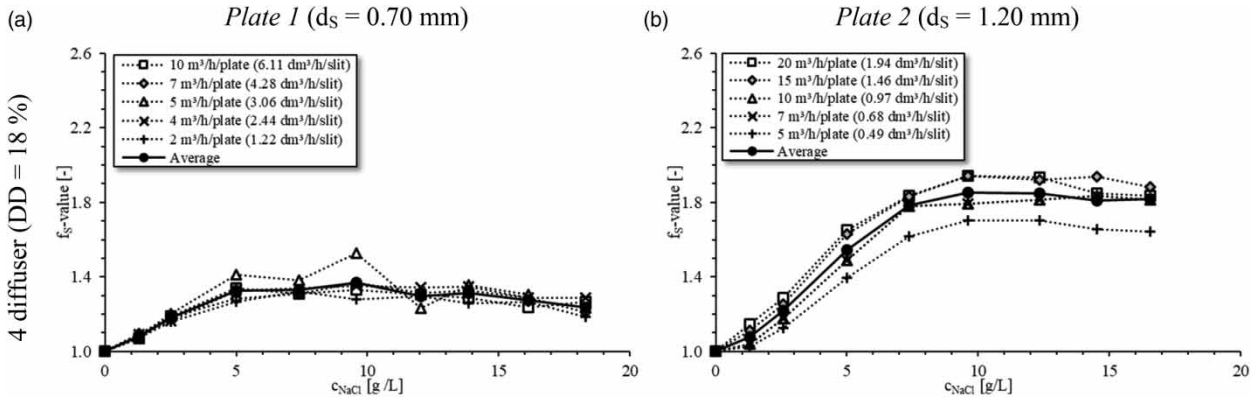

Figure 4 | f_S-values as function of c_{NaCl} from plate diffusers for different $q_{A,Plate}$ and $q_{A,Slit}$.

slits. In comparison, k_La_{20}-values in TW are in a comparable range for both diffusers (Annex 3). In addition, the clear dependency between airflow rate and f_S observed for the disc diffusers cannot be observed for *Plate 1*, in contrast to *Plate 2* (see Figure 4(b)). Here, the f_S-value increases with increasing airflow rate without reaching a noticeable peak, which is consistent with the results of the tests with 32 disc diffusers. However, as before with the disc diffusers, the operational range for *Plate 2* (25–35 m^3/h/plate) specified by manufacturer was not fully reached due to the limited blower capacity. Therefore, it can be expected, similar to the tests with the 32 disc diffusers, that with increasing airflow rate f_S would first increase further, reach a maximum and then decrease again. If the f_S value is plotted against the airflow rate, this is confirmed, as we will show below.

Results from tube diffuser

In Figure 5, f_S-values from test series with tube diffusers are plotted against c_{NaCl} for different airflow rates. For both tube diffusers, f_S increases up to 10 g/L NaCl as with the disc diffusers until $f_{S,max}$ is reached. Therefore, the results confirm the CCC_{NaCl} determined in the lab-scale experiments once again. The present data show that the average $f_{S,max}$ of *Tube 1* (2.1) is 10% higher than that of *Tube 2* (1.9), regardless of the number of installed diffusers. No effect of the number of installed diffusers (or diffuser density) on f_S, in THE case of tube diffusers, was detected. In comparison, k_La_{20}-values in *TW* are comparable for both diffusers (Annex 4). Thus, the higher f_S values could be reached with the diffusers with smaller slits, which corresponds to the results of disc diffusers.

At a salt concentration of 13 g/L NaCl and a $Q_{A,VAT}$ = 1 Nm^3/m^3/h, a $SOTR_{VAT}$ of 156 and 182 g/m^3/h could be achieved with 6 and 10 *Tube 1* diffusers respectively. This corresponds to an increase of 7% (146 g/m^3/h) and 9% (167 g/m^3/h) using *Tube 2* diffusers. Compared to $SOTR_{VAT}$ in TW it is an increase of 79% (6 tube diffusers: 87 g/m^3/h) and 84% (10 tube diffusers: 99 g/m^3/h). Therefore, for tube diffusers, $SOTR_{VAT}$ can always be increased by a higher number of installed diffusers independent of $q_{A,tube}$. However, as in *TW*, it is expected that the increase of $SOTR_{VAT}$ is minimal when *DD* exceeds a specific value. Behnisch *et al.* (2020) observed in TW only minor improvement in oxygen transfer for tube diffusers, when *DD* exceeds 35%.

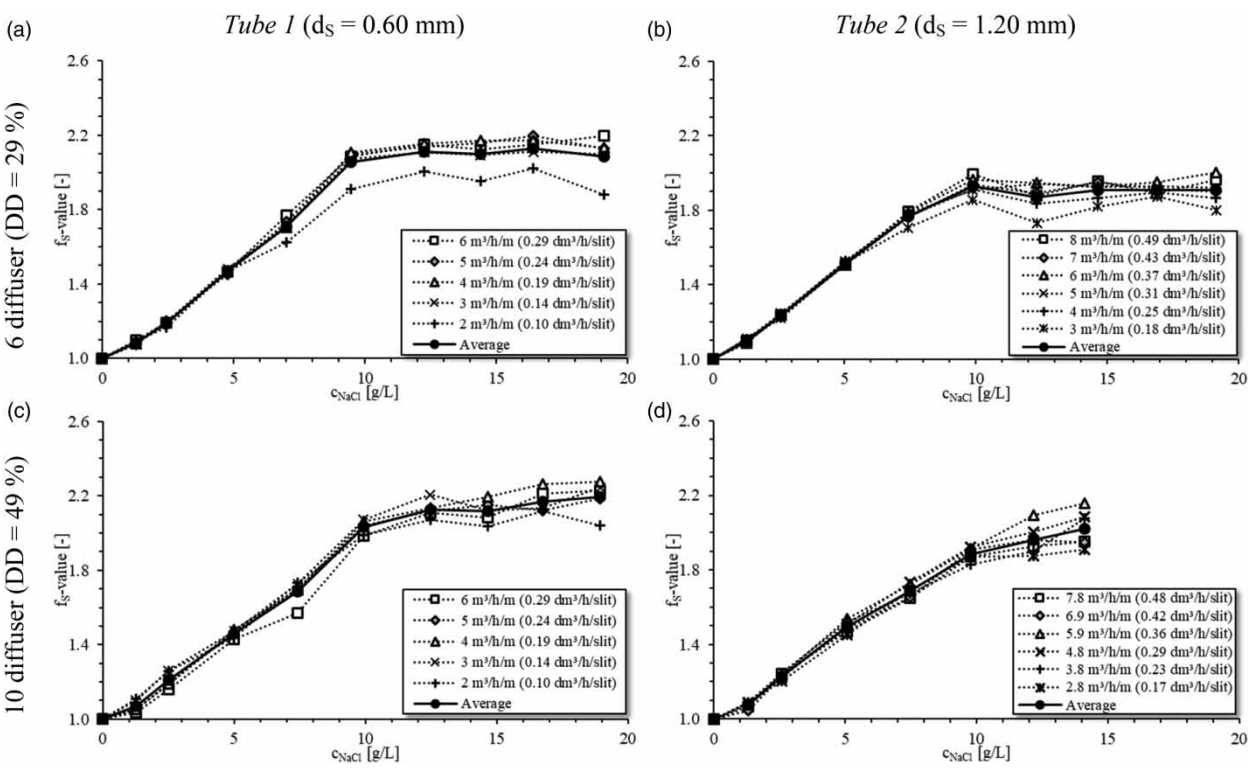

Figure 5 | f_S-values as function of c_{NaCl} from tube diffusers for different $q_{A,Tube}$ and $q_{A,Slit}$.

Dependency of f_S on airflow rate

To illustrate the dependency of $f_{S,max}$ and airflow rate for the different diffuser types, f_S as a function of the airflow rate is plotted in Figure 6. For a simplified presentation, only results of measurements are shown, where c_{NaCl} is higher than CCC_{NaCl} and f_S is constant. The airflow rate is given as the airflow rate per slit and slit length ($q_{A,dS} = q_{A,Slit} \cdot (d_S)^{-1}$). This enables a comparison between the different diffusers, which have different membrane design properties (i.e. d_S, *SD*, number of slits). It should be noted, however, that this does not take into account the elasticity of the slits, which expand depending on different material properties of the membrane (e.g. deflection, flexibility, thickness) with increasing $q_{A,Slit}$ (Loubière & Hébrard 2003). However, the expansion is very small despite high airflow rates as shown in experiments with multi-orifice diffuser membranes (Painmanakul *et al.* 2004). Therefore, the expansion of the slits with rising airflow rate is ignored here.

Figure 6 illustrates the difference between the individual diffusers. While for tube diffusers $q_{A,dS}$ is very low (0.1–0.5 dm^3/h/mm) and for disc diffusers and *Plate 2* moderate (up to 2 dm^3/h/mm), $q_{A,dS}$ for *Plate 1* is very high (1.7–9 dm^3/h/mm). The reason for this is the combination of the very low number of slits of *Plate 1* (low SD) with relatively high $q_{A,Plate}$ values. Therefore, for a better illustration of the results of the tube and disc diffusers as well as *Plate 2* diffuser, in Figure 6 the range $q_{A,dS}$ from 0 to 2 dm^3/h/mm is shown enlarged.

As mentioned before, Figure 6 shows that there is no dependency between f_S and airflow rate for tube diffusers within the considered range of airflow rate. A slight effect on f_S can be seen for *Plate 1*. In contrast, the effect is very strong for disc diffusers and *Plate 2*. For both disc diffusers as well as for *Plate 2*, the highest f_S values were reached at ~1 dm^3/h/mm. If the airflow rate changes, f_S decreases again. Sander *et al.* (2017) attribute the dependency between f_S-value and airflow rate to the fact that at low airflow rates, coalescence also occurs less frequently in TW because of the isolated bubble rise behaviour. Baz-Rodríguez *et al.* (2014) also observed no dependence between k_La and c_{Salt} when gas hold-up or airflow rate is very low and the bubbles are relatively far from each other. The decrease of f_S at very high airflow rates is explained by an increase in initial bubble size (Sander *et al.* 2017). Several experiments show that the initial bubble size increases with rising airflow rate (Loubière *et al.* 2003; Painmanakul *et al.* 2004; Hasanen *et al.* 2006). Since the bubble size remains constant during the entire ascent in a coalescence-inhibited system (Baz-Rodríguez *et al.* 2014; Behnisch *et al.* 2018), the oxygen transfer and thus f_S decreases.

When looking at the results of *Plate 1*, it has to be taken into account that the *SD* of *Plate 1* is very low (0.88 slits per cm^2) compared to *Plate 2* (5.5 slits per cm^2) and *Disc 1* and *Disc 2* (15.5 and 10 slits per cm^2). This results in distances between the slits (P_R/d_S and P_S/d_S; see Table 1) being up to nine times larger than for the other diffuser types. To prevent coalescence close to the diffuser (in TW), Painmanakul *et al.* (2004) recommend a distance between the slits in relation to the bubble size of 1.0 (i.e. $P_R/d_{32,min}$ and $P_S/d_{32,min} > 1.0$). The $d_{32,min}$ value of *Plate 1* was not measured. If we assume a $d_{32,min}$ between 1 and 2 mm, this ratio will be exceeded by more than four to nine times in the case of *Plate 1*. Therefore, no or less coalescence occurs also in TW. In addition, $q_{A,dS}$ increases very rapidly with increasing $q_{A,Plate}$ and so does the initial bubble size. Both effects lead

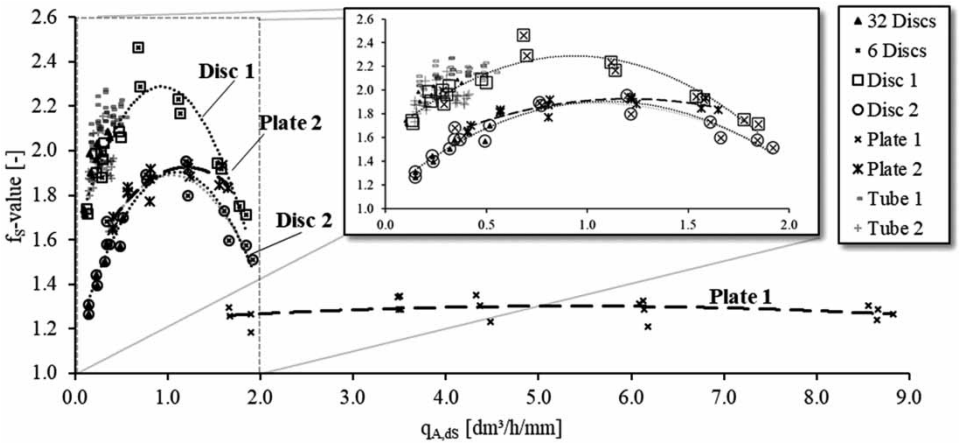

Figure 6 | f_S-value as a function of the airflow rate per slit and slit length ($q_{A,dS}$) for different diffuser types and $c_{NaCl} > CCC_{NaCl}$.

to the fact that the coalescence behaviour as well as the bubble size distribution might differ fundamentally from the other diffusers. However, the slight influence of airflow rate on f_S for *Plate 1* and the lower *CCC* cannot be explained finally on the basis of the present results. Therefore, further experiments are necessary.

For the missing dependency of f_S on airflow rate for tube diffusers, there are in our opinion three possible explanations, which we will discuss in more detail below.

- The material: Unlike the plate and disc diffusers made of EPDM, the tube diffusers are made of silicon. However, the material properties only influence the initial bubble size (Loubière & Hébrard 2003) but should not affect the coalescence behaviour of the rising bubble. Hence, the missing dependency of f_S values on airflow rate cannot be explained by the membrane material.
- Low $q_{A,dS}$ values: The number of slits per tube diffuser is much higher than for the other two diffuser types. Therefore, maximum $q_{A,dS}$ for tube diffusers (0.49 dm^3/h/mm) is very low compared to disc diffusers (1.9 dm^3/h/mm) and *Plate 2* diffuser (1.6 dm^3/h/mm). Initial bubble size should therefore change only slightly. The decrease of f_S observed for disc diffusers and *Plate 2* with increasing airflow rate is therefore missing. In contrast to the maximum $q_{A,dS}$, the achieved minimum $q_{A,dS}$ compares well with values for disc and tube diffusers (~0.14 dm^3/h/mm). The missing decrease of f_S with decreasing airflow rate can therefore not be explained by different $q_{A,dS}$ values.
- The coalescence behaviour: as described previously, for disc diffusers f_S decreases at low airflow rates because coalescence also occurs less frequently in TW due to the isolated bubble rise behaviour. The slits of tube diffusers are on the side of the diffuser and therefore the bubble formation occurs tangentially to the diffuser membrane and not vertically, as for disc and plate diffusers. Furthermore, this arrangement of the slits makes the cross-section of the assumed flow channel along the rising bubble swarm much thinner than with disc and plate diffusers (Figure 1). While the cross section of the flow channel for discs and plates roughly corresponds to the perforated membrane area, this is not the case for tubes. Here, the cross section of the flow channel corresponds to the projected surface area of the tube diffuser ($A_P = 665$ cm^2 per diffuser), which is much smaller than the active (perforated) membrane area ($A_A = 1{,}450$ cm^2 per diffuser). If the number of slits is related to A_P of the tube diffuser, the resulting quasi-slit-densities (26 and 33 slits/cm^2) are more than twice as high as the *SD* of disc and plate diffusers. Therefore, it is obvious that for tube diffusers, even at relatively low airflow rates, the bubbles are not ascent isolated and coalesce continuously in TW. This results in high f_S values even at low airflow rates.

Dependency of f_S on diffuser density

After discussing the effect of airflow rate on f_S, we checked if there was any influence of the number of installed diffusers (or DD) on f_S. According to results from Figure 5(a) and 5(c) as well as Figure 5(b) and 5(d), there is no effect of the number of installed diffusers on f_S in the case of tube diffusers. Regardless of the number of installed diffusers, the same $f_{S,max}$ was achieved as CCC_{NaCl} was reached. In the case of disc diffusers, a comparison between the different diffuser densities is more difficult, because of the overlapping influence of the airflow rate. Considering individual results of the disc diffusers in Figure 6, the same f_S could be achieved with both 6 and 32 disc diffusers for the same disc diffuser and the same $q_{A,dS}$ (or $q_{A,Disc} = (q_{A,dS}) \cdot d_S \cdot$ slits per diffuser). Hence, for 32 disc diffusers, the increase of f_S with increasing $q_{A,dS}$ is identical to that for 6 disc diffusers. Due to the high number of diffusers and limited blower capacity, the range of tested airflow rates with 32 disc diffusers is significantly below the tests with 6 disc diffusers or the given specified operating range from manufacturers. If $q_{A,dS}$ and $q_{A,Disc}$ continue to increase, a similar dependency between f_S and $q_{A,dS}$ (or $q_{A,Disc}$) will most likely result as was shown for the tests with 6 disc diffusers. Therefore, no influence of diffuser density on f_S for disc diffusers as well as for tube diffusers was detectable. For plate diffusers only one diffuser density was tested. A comparison is therefore not possible. The result that diffuser density has no effect on f_S promotes the notion that bubbles only coalesce with bubbles from the same diffuser or adjacent slits and not with bubbles from other diffusers. This confirms the observations of Hasanen *et al.* (2006) and Behnisch *et al.* (2018), that coalescence occurs mainly close to the diffuser.

Summarize effects on f_S

The results shown above correspond to the results from Part I of this paper: Both c_{Salt} as well as the design of the diffuser membrane (see Table 1) have an influence on k_La or f_S in SW (Behnisch *et al.* 2018). Hence, at high c_{Salt} diffusers with smaller detaching bubbles show higher f_S and k_La values. Additionally, we could show that the type of the

diffuser also influences the oxygen transfer in SW. For tube diffusers, f_S only depends on c_{Salt}, while for disc and plate diffusers f_S also depends on $q_{A,Disc}$ and $q_{A,Plate}$ respectively. Except *Plate 1*, for all diffusers $f_{S,max}$ was reached when $c_{Salt} \geq CCC$. Furthermore, diffuser density does not seem to affect f_S.

Additional design considerations

Other factors also have to be taken into account for design of aeration systems in SW. An important parameter is c_S, which decreases with increasing c_{Salt} (Annex 1). Due to the lower concentration gradient between gas and liquid phase and reduced molecular diffusivity, k_L is expected to decrease, resulting in a lower f_S and k_La. When looking at the results of plate and tube diffusers (Figures 4 and 5), we did not observe a significant decrease in f_S after reaching its peak value in the considered concentration range. Because of the lower range of tested salt concentration, a clear conclusion is not possible for disc diffusers. Nevertheless, we do not expect a significant decrease of f_S for disc diffusers with further increasing c_{Salt}. This is confirmed by the results of Baz-Rodríguez *et al.* (2014), who found no dependence of k_La, a and k_L on c_{Salt} when coalescence is completely inhibited. They show that the reduction of the molecular diffusivity with increasing c_{Salt} and the effect on k_L is marginal. According to these authors, the main effect on k_L is the slip velocity, which is substantially influenced by the bubble size (i.e. d_{32} or a). However, the reduced c_S also decrease $SOTR_{VAT}$ and *SSOTE*, as shown in Figure 7(a). Similar to f_S, *SSOTE* increases with increasing c_{NaCl} until a maximum is reached. *SSOTE* of up to 15%/m could be reached. Diffusers with the smaller slits (*Tube 1*, *Disc 1*) always exhibit higher values than diffusers with larger slits (*Tube 2*, *Disc 2*). In TW, *SSOTE* increases with increasing diffuser density (Behnisch *et al.* 2020). When comparing the results of 6 and 10 *Tube 1* diffusers, the same can be observed in SW. When reaching the peak value, *SSOTE* slightly decreases as a result of the reduced c_S. The decrease averages about 0.7%/m for $c_{NaCl} = 20$ g/L compared to the peak value at $c_{NaCl} = CCC_{NaCl}$. Nevertheless, SW *SSOTE* still outperforms *SSOTE* values that can be achieved in TW with conventional fine-bubble diffusers (8.5–9.8%/m), even at very high diffuser densities (Behnisch *et al.* 2020).

Another factor that must be considered in the design of aeration systems is the total air supply pressure (p_T), which includes the hydrostatic pressure resulting from depth of submergence (p_h), pressure drop of pipes and valves (p_s) and pressure drop of diffusers (p_d) (Krampe 2011). The p_h increases with increasing c_{Salt} due to the increment of water density. Nevertheless, in practice this increase can be neglected. The density of water rises marginally by 1.6% with an increase in c_{NaCl} from 0 g/L (997 kg/L at 20 °C) to 20 g/L (1.013 kg/L at 20 °C). The p_S is not affected by c_{Salt}. Also no dependence against c_{Salt} was found for p_d (Annex 5). Nevertheless, when improving the oxygen transfer in

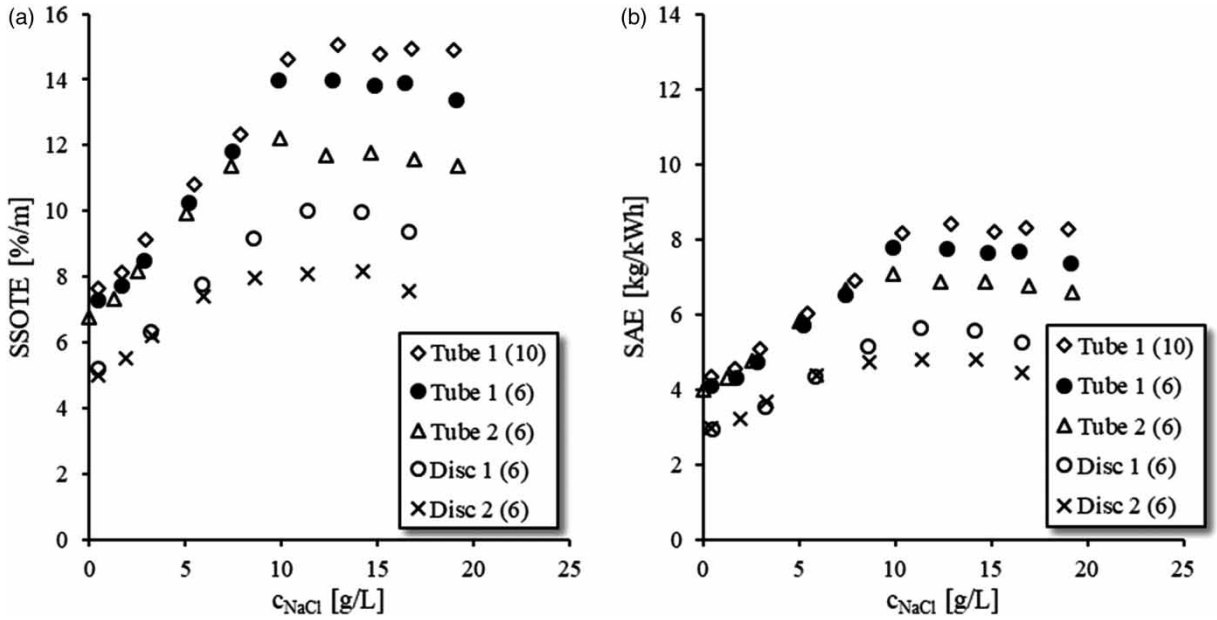

Figure 7 | Average *SSOTE* values as function of c_{NaCl} (a); average *SAE* values as a function of c_{NaCl} (b) calculated with isochoric power formula ($\eta = 0.60$).

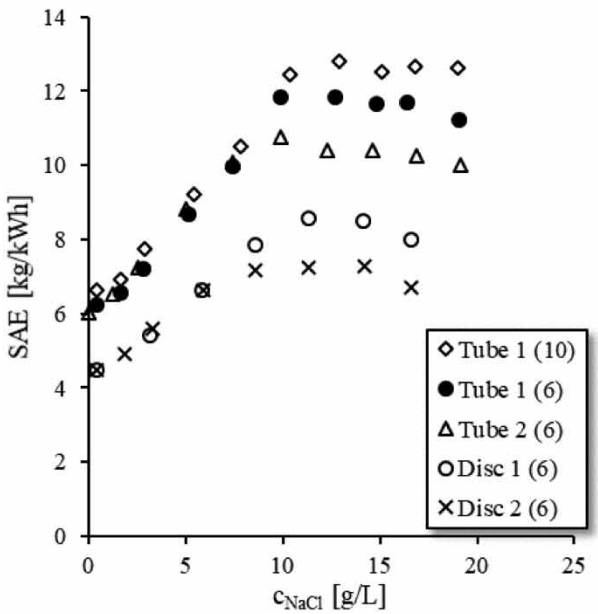

Adiabatic power formula according to Metcalf et al. (2014):

$$P = \frac{Q_A \cdot \rho \cdot R \cdot T_0}{28.97 \cdot \frac{k-1}{k} \cdot \eta} \cdot \left[\left(\frac{p_0 + p_T}{p_0} \right)^{\frac{k-1}{k}} - 1 \right]$$

With:

P = power requirement [kW]

Q_A: airflow rate [m³/s]

ρ: air density (=1.20 kg/m³ with T = 20 °C)

R: universal gas constant = 8.314 J/(mol·K)

T_0: absolute inlet temperature (=293 K)

p_0: absolute inlet pressure (=101.3 kPa)

p_T: air supply pressure [kPa]

k: specific heat ratio (=1.395)

28.97: molecular weight of dry air

η: overall efficiency (= 0.80 for turbo blowers)

Figure 8 | Average *SAE* values with $\eta = 0.80$ (left) calculated with adiabatic power formula (right).

SW by installing diffusers with smaller slits, p_d increases. In our tests, for tube and disc diffusers the difference in p_d between the diffuser with the smaller slits and those with the larger slits was on average 2.2 kPa (at the same q_A, see Annex 5). Thus, in SW, a higher f_S tends to go hand in hand with a higher p_d and therefore p_T. The increased p_T results in a higher power requirement (P) for the blowers.

When calculating P, we must differentiate between isochoric compression and adiabatic compression. Positive displacement blowers (as used here) are widely used in WWTP. Since they compress a fixed volume of air in an enclosed space to a higher pressure, they operate using the isochoric compression principle (Mueller *et al.* 2002). P can be calculated according to the following formula: $P = Q_A \cdot p_T/\eta$; η being the overall efficiency of the blower. For our calculation, we assumed a typical η of 0.60 (Bell & Abel 2011). Then we calculated the standard aeration efficiency ($SAE = SOTR/P$).

With *SAE*, we are able to illustrate the interaction between increased energy demand due to increased p_T through the smaller slits and the improved oxygen transfer. The average *SAE* is shown in Figure 7(b) as a function of c_{NaCl}. Since identical Q_A were set for each diffuser type, its influence on *SAE* is eliminated and the average values are sufficient for a comparison. Figure 7(b) shows that SAE in TW ranges between 3.0 and 4.4 kg/kWh and thus within an expected range for such a kind of operation conditions (Behnisch *et al.* 2020). With increasing c_{Salt} *SAE* increases and reaches its peak value, similar to *SSOTE*. *SAE* for the diffusers with smaller slits (*Tube 1*, *Disc 1*) are comparable or higher than for the diffusers with larger slits (*Tube 2*, *Disc 2*). Hence, with *Tube 1* (smaller slits) *SAE* of up to 8.4 kg/kWh could be achieved.

Contrary to positive displacement blowers, with turbo blowers internal air compression takes place (= adiabatic compression). Turbo blowers are generally designed for large airflow rates and are therefore used especially on large WWTP. P depends upon the inlet pressure (p_0), air density (ρ) and inlet temperature (T_0) (Mueller *et al.* 2002). Depending on design and operation conditions, overall efficiencies for turbo blowers of up to 0.85 are possible (Bell & Abel 2011). In order to consider these types of blowers as well, we calculated *SAE* again using the adiabatic power formula (EPA 1989). All results and the formula with the assumed operating conditions are shown in Figure 8. Due to the higher overall efficiency (using a constant η of 0.80) and the chosen operation conditions ($T_0 = 20$ °C; $p_0 = 101.3$ kPa; $\rho = 1.2$ kg/m³), on average 52% higher SAE values of up to 12.8 kg/kWh were achieved compared to positive displacement blowers. However, it has to be taken into account that the presented power requirement values are only based on theoretical calculations. Since overall efficiency and the power requirement will change under varying operation conditions, lower *SAE* values are likely to be achieved in practice. Apart from that, the previous conclusions remain valid. Higher *SAE* values were achieved with diffusers with smaller slits.

In summary, the *SAE* results show that, independent of the blower type used and despite the higher pressure drop, in SW higher efficiency of the aeration system is achieved using the diffusers with smaller slits. However, it is questionable whether this can be applied to all diffusers. Whether a diffuser with smaller slits in SW ensures a more efficient aeration depends largely on the difference in oxygen transfer as well as on pressure drop compared to the diffuser with larger slits. Additionally, further measurements need to show whether a higher SAE value can also be achieved in activated sludge. The activated sludge could have an influence on the coalescence behaviour in the aerated tank. Diffusers with smaller slits could also lead to increased fouling. Therefore, further experiments are already planned to answer these questions.

CONCLUSION

In the present work, the experiments presented in Part I of this paper (Behnisch *et al.* 2018) were continued to investigate the oxygen transfer of fine-bubble aeration systems and their influencing factors in saline water. In Part I, data from bubble size distribution were combined with results from oxygen transfer tests to investigate the impact of the design of the diffuser membrane. Within Part II, the effect of different salts as well as the effects of diffuser type and density on oxygen transfer of fine-bubble aeration systems in saline water is presented.

First, we determined the critical coalescence concentration (*CCC)* for various salts for the first time using conventional fine-bubble diffusers, for which we developed a new analytical approach. When *CCC* is reached, coalescence is completely inhibited and k_La_{20} and f_S remain constant. Regardless of salt type, the $f_{S,max}$ values reached were the same. With the new analytical approach, the *CCC* is determined by evaluating the oxygen transfer rate at different salt concentrations. The new method is much faster and easier to use than bubble size measurement and provides valid results. In the future, this will make it possible to investigate the coalescence behaviour for any aeration system and (mixed) salt solution quickly and easily. Furthermore, since salt and salt mixture in wastewater change and depend on the origin of the used water, we recommend that in the future not only the total salt concentration should be considered in wastewater analytics but also its composition from different salts (e.g. by ion analysis).

Second, we carried out oxygen transfer tests with three different types of diffusers at different diffuser densities in a pilot-scale test tank at a water depth of 3.8 m and at different NaCl concentrations. The effect of the design of the diffuser membrane observed in Part I was confirmed. Except for *Plate 1*, diffuser membranes with smaller detaching bubbles show higher f_S values. Furthermore, our results show that there is a clear influence of the diffuser type. While f_S for tube diffusers only depends on the salt concentration, the other diffuser types show a clear influence of the airflow rate per slit and slit length ($q_{A,dS}$). For disc diffusers and *Plate 2*, the highest f_S values were achieved at $q_{A,dS} \sim 1.0\ dm^3/h/mm$. If $q_{A,dS}$ changes, f_S and k_La will decrease again. This complicates the operation of an aeration system. When using tube diffusers, this problem can be avoided. To achieve a high oxygen transfer in saline water, the slit density of the diffuser membrane can be further increased. In tap water, the slit density is usually up to 15 slits per cm^2 to prevent coalescence close to the diffuser. Under saline conditions ($c_{Salt} > CCC$), the coalescence is inhibited and the slit density can be increased further. This also prevents high $q_{A,dS}$ and thus an increase in initial bubble size.

Third, despite the reduced oxygen saturation concentration in saline water, extremely high *SSOTE* values compared to tap water of up to 15%/m were achieved during the tests in the pilot-scale test tank. *SSOTE* are much higher than is possible with conventional fine-bubble diffusers in tap water. Using isochoric power formula (valid for positive displacement blowers), calculated *SAE* values of up to 8.4 kg/kWh show that by using diffusers with smaller slits, the energy efficiency of the aeration system will improve in saline water despite the increased pressure drop. If even more efficient blowers (e.g. turbo blowers) were used, theoretically (using adiabatic power formula) even higher *SAE* of up to 12.8 kg/kWh values could be achieved. However, it is not yet known whether the use of diffusers with smaller slits also improves aeration in activated sludge tanks. The coalescence behaviour in the aerated tank as well as the fouling of the diffusers could be influenced by the activated sludge. Therefore, further investigations are already planned.

ACKNOWLEDGEMENTS

We thank the German Federal Ministry of Education and Research (BMBF) for funding the research project WaReIp 'Water-Reuse in Industrial Parks' (Grant No. 02WAV1409A).

DATA AVAILABILITY STATEMENT

All relevant data are included in the paper or its Supplementary Information.

REFERENCES

ASCE/EWRI 18-18 2018 *Standard Guidelines for In-Process Oxygen Transfer Testing (ASCE/EWRI 18-18)*. American Society of Engineers, Reston, VA.

Baz-Rodríguez, S. A., Botello-Álvarez, J. E., Estrada-Baltazar, A., Vilchiz-Bravo, L. E., Padilla-Medina, J. A. & Miranda-López, R. 2014 Effect of electrolytes in aqueous solutions on oxygen transfer in gas-liquid bubble columns. *Chemical Engineering Research and Design* **92** (11), 2352–2360.

Behnisch, J., Ganzauge, A., Sander, S., Herrling, M. P. & Wagner, M. 2018 Improving aeration systems in saline water: measurement of local bubble size and volumetric mass transfer coefficient of conventional membrane diffusers. *Water Science and Technology* **78** (3–4), 860–867.

Behnisch, J., Schwarz, M. & Wagner, M. 2020 Three decades of oxygen transfer tests in clean water in a pilot scale test tank with fine-bubble diffusers and the resulting conclusions for WWTP operation. *Water Practice and Technology* **15** (4), 910–920.

Bell, K. Y. & Abel, S. 2011 Optimization of WWTP aeration process upgrades for energy efficiency. *Water Practice and Technology* **6** (2).

Cho, Y. S. & Laskowski, J. S. 2002 Effect of flotation frothers on bubble size and foam stability. *International Journal of Mineral Processing* **64** (2–3), 69–80.

Craig, V. S. J., Ninham, B. W. & Pashley, R. M. 1993 Effect of electrolytes on bubble coalescence. *Nature* **364** (6435), 317–319.

EN 12255-15 2003 *Wastewater Treatment Plants – Part 15: Measurement of the Oxygen Transfer in Clean Water in Aeration Tanks of Activated Sludge Plants*.

EPA 1989 *Design Manual – Fine Pore Aeration Systems (EPA/625/1-89/023)*. U.S. Environmental Protection Agency, Washington, DC, USA.

Firouzi, M., Howes, T. & Nguyen, A. V. 2015 A quantitative review of the transition salt concentration for inhibiting bubble coalescence. *Advances in Colloid and Interface Science* **222**, 305–318.

Grau, R. A., Laskowski, J. S. & Heiskanen, K. 2005 Effect of frothers on bubble size. *International Journal of Mineral Processing* **76** (4), 225–233.

Hasanen, A., Orivuori, P. & Aittamaa, J. 2006 Measurements of local bubble size distribution from various flexible membrane diffusers. *Chemical Engineering and Processing* **2006** (45), 291–302.

He, H., Chen, Y., Li, X., Cheng, Y., Yang, C. & Zeng, G. 2017 Influence of salinity on microorganisms in activated sludge processes: a review. *International Biodeterioration & Biodegradation* **119**, 520–527.

ISO 5814 2012 *Water Quality – Determination of Dissolved Oxygen – Electrochemical Probe method*.

Krampe, J. 2011 Assessment of diffuser pressure loss on WWTPs in Baden-Württemberg. *Water Science and Technology* **62** (12), 3027–3033.

Lefebvre, O. & Moletta, R. 2006 Treatment of organic pollution in industrial saline wastewater: a literature review. *Water Research* **40** (28), 3671–3682.

Lessard, R. R. & Zieminski, S. A. 1971 Bubble coalescence and gas transfer in aqueous electrolytic solutions. *Industrial & Engineering Chemistry Fundamentals* **10** (2), 260–269.

Loubière, K. & Hébrard, G. 2003 Bubble formation from a flexible hole submerged in an inviscid liquid. *Chemical Engineering Science* **58** (1), 135–148.

Loubière, K., Hébrard, G. & Guiraud, P. 2003 Dynamics of bubble growth and detachment from rigid and flexible orifices. *The Canadian Journal of Chemical Engineering* **81** (3–4), 499–507.

Marrucci, G. & Nicodemo, L. 1967 Coalescence of gas bubbles in aqueous solutions of inorganic electrolytes. *Chemical Engineering Science* **22** (9), 1257–1265.

Metcalf, E., Tchobanoglous, G., Abu-Orf, M., Stensel, H. D., Bowden, G. & Pfrang, W. 2014 *Wastewater Engineering. Treatment and Resource Recovery*, 5th edn. McGraw-Hill, New York, NY.

Mueller, J. A., Boyle, W. C. & Pöpel, H. J. 2002 *Aeration. Principles and Practice*, Vol. 11. CRC Press, Boca Raton, FL.

Painmanakul, P., Loubiere, K., Hebrard, G. & Buffiere, P. 2004 Study of different membrane spargers used in waste water treatment: characterisation and performance. *Chemical Engineering and Processing: Process Intensification* **43** (11), 1347–1359.

Prince, M. J. & Blanch, H. W. 1990 Transition electrolyte concentrations for bubble coalescence. *AIChE J.* **36** (9), 1425–1429.

Quinn, J. J., Sovechles, J. M., Finch, J. A. & Waters, K. E. 2014 Critical coalescence concentration of inorganic salt solutions. *Minerals Engineering* **58**, 1–6.

Rusydi, A. F. 2018 Correlation between conductivity and total dissolved solid in various type of water: a review. *IOP Conference Series: Earth and Environmental Science* **118**, 12019.

Sander, S. 2018 *Optimierung der Bemessung feinblasiger Druckbelüftungssysteme bei erhöhten Meersalzkonzentrationen* (*Optimisation of the design of fine-bubble aeration systems at increased sea salt concentrations*). Darmstadt (IWAR Schriftenreihe, 243).

Sander, S., Behnisch, J. & Wagner, M. 2017 Design of fine-bubble aeration systems for municipal WWTPs with high sea salt concentrations. *Water Science and Technology* **75** (7), 1555–1563.

Sovechles, J. M. & Waters, K. E. 2015 Effect of ionic strength on bubble coalescence in inorganic salt and seawater solutions. *AIChE Journal* **61** (8), 2489–2496.

Wagner, M. & Stenstrom, M. K. 2014 Aeration and mixing. In: *Activated Sludge – 100 Years and Counting* (D. Jenkins & J. Wanner, eds). IWA Publishing, London, UK, pp. 131–153.

Wagner, M., Pöpel, H. J. & Kalte, P. 1998 Pure oxygen desorption method – a new and cost-effective method for the determination of oxygen transfer rates in clean water. *Water Science and Technology* **38** (3), 103–109.

Zlokarnik, M. 1980 Koaleszenzphänomene im System gasförmig/flüssig und deren Einfluss auf den O_2-Eintrag bei der biologischen Abwasserreinigung (Coalescence phenomena in the gas/liquid system and their influences on oxygen uptake in biological waste water treatment). *Korrespondenz Abwasser, Abfall* **27** (11), 728–734.

First received 22 February 2021; accepted in revised form 27 April 2021. Available online 11 May 2021